ICONHIC2022
3rd International Conference on Natural Hazards & Infrastructure
5-7 July 2022, Athens, Greece

Analytical vulnerability-based risk assessment of school systems exposed to multi-hazards

Ahsana Parammal Vatteri [1], Dina D'Ayala
University College London

Pierre Gehl
BRGM, France

ABSTRACT

Concurrent effects of floods and earthquakes pose significant risk to the vulnerable population of students and their education process. Yearly flood events with low inundation depths may not cause structural damage, however, resulting material degradation contribute to higher vulnerability to subsequent seismic events. This recurring damage, combined with other functional losses, ultimately result in disruption to education delivery. The socio-economic condition of the users-community also plays a role in the extent of such disruption. A complex problem of this nature demands consideration of a large number of dimensions, to estimate the impact to the school system infrastructure in a locality. To handle the qualitative and quantitative nature of these variables, a Bayesian network (BN) model is proposed representing multiple schools in a locality as a system. Three factors are considered to contribute to the system disruption, namely, schools' physical functionality loss from damage to infrastructure, accessibility and use loss, and social vulnerability. The impact is quantified through the probability of the system being in various states of disruption. The general methodology is illustrated by a case-study of school buildings in Guwahati, India, whereby the majority of buildings is constructed in confined masonry with varying level of seismic performance. The results, produced in terms of probability of system disruption, can support decision-making and strategic planning in the face of multiple hazards.

Keywords: Education disruption, multi-hazard vulnerability assessment, School systems, Bayesian Networks

BACKGROUND

Multi-hazard risk assessment of the built environment is an integral part of disaster risk reduction from natural hazards. This is particularly relevant for critical infrastructure, including schools in locations exposed to multiple hazards such as earthquakes and floods. In addition to individual hazards, increasing evidence from around the world is highlighting the necessity of considering consecutive or sequential hazards in the assessment of disaster risk (de Ruiter et al. 2020a), as the effects of a hazard event overlaps with the effects of another in overlapping space and time windows. Hence, techniques for assessing the performance of buildings under multiple hazards is highly encouraged by the Sendai Framework (UNISDR 2015) to ensure safe schooling facilities.

Large earthquakes and frequent floods cause physical damage to school infrastructure and cause interruption to the education process, as frequently observed from past events. Evidence from the past 30 years (Spitak M_s 6.8 (1988) to Indonesia M_w 7.5 (2018)) reports seismic collapse and damage of school buildings, resulting in casualties and disruption to schooling for long periods (UN 2009, Miyamoto and Gilani 2017, Pribadi et al.

[1] Corresponding Author: Ahsana Parammal Vatteri, University College London, UK, ahsana.vatteri.17@ucl.ac.uk

2021). School children are thus identified as a most vulnerable population in earthquakes (UN 2009), while it is recognised that school architecture renders these buildings particularly prone to damage from earthquakes (Rodgers 2012). While disruptive earthquakes are rare events, floods are the most common natural hazard in the world (Doocy et al. 2013). Recurring floods disrupt education by causing physical damage to the school infrastructure, affecting the organisational structure, requiring the use of schools as temporary shelters and negatively affecting wellbeing of individuals and communities (Forino and Meding 2018). Persistent issues of disruption to education associated with flooding are reported worldwide, including Kenya (Akello 2014), Zimbabwe (Mudavanhu 2014) and Philippines (Ardales et al. 2016). During the South-Asian floods of 2017, more than 18000 schools were damaged in the north and north-east of India, Nepal and Bangladesh (Savethechildren.org.uk, 2017), affecting over 1.8 million children. Closure of schools for long periods often leads to high rates of education drop-out, especially in poor communities and when schools are used as shelters (Munsaka and Mutasa 2020). The period of disruption to education is found to vary widely after disasters, for example, it often takes many weeks and even months for the schools to resume full operation after a heavy flood event in India (Bertho et al. 2012; BBC 2015; Reliefweb 2018).

Schools being an integral part of any community, social vulnerability of the community affects the performance of schools, especially in the face of damaging and disruptive events. It is observed that socially vulnerable communities disproportionately receive the negative impacts of natural hazards (de Ruiter et al. 2020b). A number of factors are identified to influence the social vulnerability of a community, including economic status, education level, age, disabilities, minority status or vulnerable groups, housing type, access to transportation etc. (Flanagan et al. 2011, Utami 2019, Fatemi et al. 2017). Social vulnerability status also affects the use schools for immediate evacuation and sheltering of displaced people. Even though such use is controversial many countries including India, Philippines, Japan, Fiji etc., (Asia Pacific Coalition for School Safety 2017, (APCSS 2017)), use schools as evacuation shelters in emergencies. Prolonged and beyond capacity use of schools as shelters cause damage to buildings and service lines, further delaying the education process and quality (APCSS. 2017). Hence, the social vulnerability factor should be given due attention in disaster management and risk reduction programmes, and more importantly in the context of school infrastructure and disruption to education.

Development of tools to cater for multi-hazard risk assessment that incorporate structural and non-structural elements of the school infrastructure system is hence a necessity of the hour. Bayesian networks (BN) is one such tool that is suitable to integrate quantitative and qualitative information to a complex system model (Wu et al. 2019). This paper proposes a BN framework for risk assessment of the school system in a district (a set of several schools of different capacity and schooling level) from sequential flood and seismic hazards, in terms of overall disruption to school education delivery to the community that it serves. The framework integrates loss of functionality of schools from: 1) physical fragility of CM buildings and 2) accessibility loss due to the hazard effects and computes the probability of different states of disruption. Additionally, influence of social vulnerability indicators on the disruption is modelled into the network, in order to study the influence on disruption probabilities when this factor is taken into account.

Case-study

The method is illustrated by application to a case-study of confined masonry school buildings in Guwahati, India. The case-study location, Guwahati city in the north-east of India, is situated in the most severe seismic hazard zone in India, i.e. zone V according to Indian Standard 1893 (IS1893 2002), and has witnessed several large earthquakes. This study adopts the hazard curves for Guwahati as proposed by Nath and Thingbaijam (2012), which suggests PGA of 0.65g and 1.36g for DBE and MCE respectively, which is higher than the IS1893 estimate. Additionally, the city is affected by annual monsoonic and fluvial floods, making it a suitable choice for a multi-hazard risk study. Flood hazard curves in terms of flood depth reported by Sahoo and Sreeja (2017) is used for this study. A desk study of school infrastructure of Guwahati city (Pathak 2014) and field visits to the location, identified that 75% of the buildings are of masonry construction, of which more than 60% are confined by reinforced concrete (RC) tie-columns and tie-beams to various extent, making this the predominant typology. These school buildings exhibit significant similarities with the engineered confined masonry typology, while also showing critical deviation from national standards. A detailed analysis of their features and classification was presented elsewhere (Vatteri and D'Ayala 2021). One of the CM typologies having minimum required confinement in the form of plinth and lintel bands, corner columns and intermediate

columns, and good connections at the interfaces of tie-columns and wall panels is chosen for the analysis in this paper.

A brief discussion on the physical fragility of CM buildings under combined flood-seismic loads and the approach adopted in this study to derive fragility curves are presented in the second section, results of which are fed into the BN framework for the school disruption assessment, developed in the third section. The last two sections present results of the BN analysis and the conclusions of the study, respectively. The framework is found helpful in combining various system factors into a probabilistic framework that can assist in decision-making and mitigation endeavours with regard to education delivery.

PHYSICAL VULNERABILITY OF CM BUILDINGS AGAINST FLOOD AND SEISMIC HAZARDS

CM typology is found to have superior seismic performance compared to unreinforced masonry (Tomaževiˇc and Weiss 2010; Chourasia et al. 2016), mainly due to improved ductility provided by the confining elements. There is extensive experimental and numerical work on seismic capacity assessment of confined masonry structures, (e.g., Tomaževič and Klemenc 1997; Brzev 2007; Meli et al. 2011; Chourasia et al. 2013, 2016; Alcocer et al. 2020). Vatteri and D'Ayala (2021) presents a comprehensive review of methods for out-of-plane and in-plane assessment of confined masonry school structures and derive a numerical analysis -based procedure for fragility assessment of selected confined masonry typologies, which is adopted in the present study.

In contrast, physically based numerical analysis of CM, let alone rdinary masonry walls subjected to flood lateral loading has received very little attention (Milanesi et al. 2018), even though floods are a common and frequently recurring hazard that causes predictable damage. Analytical assessment of lateral capacity of masonry walls under non-uniform (flood) loading is reported using the yield line approach (Kelman and Spence 2003; Herbert 2013). Applying yield line theory to masonry walls in residential buildings, Kelman and Spence (2003) concluded that the critical hydrostatic water head is about 1-1.5 m and the water depth can be as low as 0.5m when realistic flow velocity values are considered. Experimental and analytical studies by Herbert et al. (2012) on walls loaded by combined hydrostatic, hydrodynamic and uniform loads, showed that the frictional strength method gives lower ultimate water levels compared to flexural strength method and concluded that the former is not suitable for calculating strength of uncracked masonry walls. The results obtained were comparable with Kelman and Spence (2003).

Investigation on masonry buildings subjected to combined flood and seismic hazards is very rare (D'Ayala et al. 2016), even more so when considering combined effects. A few studies have examined seismic and flood effects and risk assessment in the context of disaster risk reduction, however, quantification and comparison of their effects on building vulnerability is not common (de Ruiter et al. 2020b). A comparison of empirical vulnerability assessment techniques used for seismic or flood hazards and suggest that greater homogeneization of the two fields of work is needed, using common indicators (De Ruiter et al. 2017). Dabbeek et al. (2020) estimated the combined seismic and flood losses in the Middle-East region, by adding losses estimated from individual hazards, ignoring any combined effects of the hazards. It is also noticed that vulnerability reduction measures against flood hazard alone may increase the vulnerability against earthquake hazard (de Ruiter et al. 2020b). These evidences highlight the necessity for developing techniques for combined flood-seismic vulnerability assessment of buildings.

The present study addresses the derivation of fragility curves of confined masonry buildings for comined flood-seismic hazards by employing Applied Elements Analysis on Extreme Loading for Structures (ELS) software. (ELS 2004). A brief description of the fragility derivation is presented below, while the reader is referred to Vatteri et al. (2022) (to be published) for a detailed description of the procedure and discussion of results considering a larger sample of index buildings. The ELS model of the index building (IB) in this study is generated for a single classroom using equivalent properties of unweathered masonry, as obtained from relevant literature (Kaushik et al. 2007; Choudhury and Pathak 2014). A loading regime as shown in Figure 1a is designed for this problem that simulates the condition that the representative IB has gone through several flood events in its lifetime, which has weakened the masonry properties in the lower 1m height of the masonry walls, as flood depth in Guwahati city is observed to be within 1m even for a 1 in 100 event (Sahoo and Sreeja 2017). It is assumed that the lowermost 0.5 m and the next 0.5 m of masonry have 20% and 10% reduced

properties of un-weathered masonry, respectively (Stephenson and D'Ayala 2019). A current flood event of given depth in the range of 0-1 m is applied to the IB, considering only the hydrostatic loads from flood inundation. This event being of small magnitude, i.e. below the critical water height that causes structural damage, the IB experiences deformations in the elastic range. Assuming that the two events are concurrent and sequential, a monotonically increasing ground acceleration is then applied until failure by formation of sufficient cracks to develop a failure mechanism. The ground acceleration is applied in the transverse (Y) direction, as the IB is found weaker in this direction in Vatteri and D'Ayala (2021). This process is repeated for five increments of flood depth, i.e. 0, 0.25m, 0.5m, 0.75m and 1m, followed by ground acceleration.

Figure 1b shows the capacity curves and the crack patterns at failure for the worst case of flood (1m) combined with the seismic action. The capacity curves show reduction of strength capacity (by 9%) and initial stiffness (by 25%) with increase in flood depth from zero to 1m. The displacement capacity is found to be dependent on the wall geometry in each flood increment case. Fragility curves are derived by applying N2 method (Fajfar 2000) for each increment of flood depth, against PGA as the IM, against three performance levels namely Immediate Occupancy (IO), Life Safety (LS) and Collapse Prevention (CP). The results are shown in Figure 1c. This combined analysis process thus enables probabilistic assessment of the school buildings across the intensity ranges of both hazards, illustrating its ability to capture physical effects in multi-hazard scenarios. This suite of fragility functions is used as input to the Bayesian Network in the following section, to represent the probabilistic distribution of the physical performance of the IB.

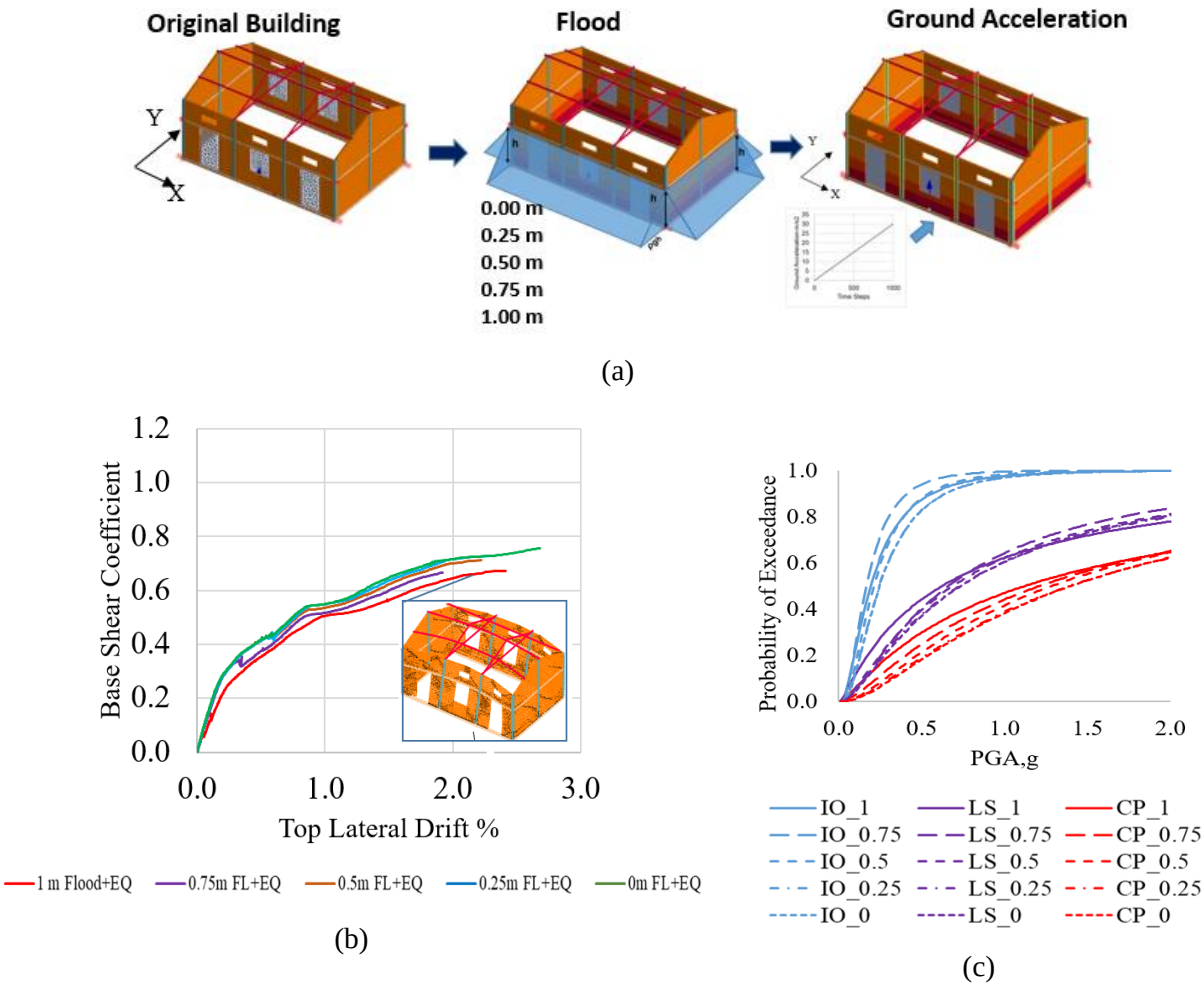

Figure 1 *a) Sequential flood-seismic loading, b) Capacity curves and c) Fragility functions for the sequential loading scenario for the index building*

The following section presents the BN framework for estimating disruption of school system considering physical fragility, accessibility loss and social vulnerability factors and their interdependencies. The subsections describe approaches for considering these factors in this framework and their quantification.

BN FOR COMBINED FLOOD AND SEISMIC VULNERABILITY ASSESSMENT

Bayesian Network (BN) allows modelling complex systems with uncertainties, to estimate system performance under described hazards' occurrence. The BN approach involves designing the network of variables in a problem, establishing their causal relationships in terms of *parent* and *child*. Each variable can have multiple states of existence and a conditional probability table (CPT) that defines the conditional probability of each state, given the states of its parent nodes (Weber et al. 2012). BN based analysis of physical infrastructure performance is a growing field of research (Bayraktarli et al. 2005; Bensi 2010; Franchin et al. 2016; Gehl 2017), as it provides an intuitive visualization of the problem in the form of a directed acyclic graph (DAG) allowing to reduce the complexity and interdependency between variables by logically shaping the network. In the context of seismic risk assessment, BNs have been applied to bridges (Franchin *et al.* 2016) and buildings (Bayraktarli et al. 2005), or entire infrastructure systems (Bensi, 2010) and for disaster management. BN is also applied for flood risk assessment, in the context of housing infrastructure (Sen et al. 2021b) and urban flood disasters (Wu et al. 2019) and Huang et al. 2021). Gehl & D'Ayala (2018) have applied BN to assess multi-hazard vulnerability of road infrastructure considering scenarios of uncorrelated and cascading hazard events including earthquakes, fluvial floods and associated ground failure.

A network of multiple schools in a region or city forms the school infrastructure of the city, providing the crucial service of education to the community. As a collection of various structural and non-structural elements that are interlinked to provide a common objective of education, school infrastructure can be considered as a system (Simonovic 2003), to which natural hazards are the external factors. This study presents the application of BN for the performance assessment of school systems in terms of disruption to education, when exposed to combined flood and seismic hazards, following the approach of Gehl and D'Ayala (2018), where the effects of sequential hazards are first characterised through fragility curves and harmonised at the functionality level of school systems. The objective is to estimate the disruption to education delivery due to reduction in structural and functional response of the buildings, and to explore the influence of social vulnerability level on the overall disruption. The BN framework estimates the probability of different periods of disruption, which may be caused by loss of school functionality from structural and non-structural damage inflicted by the hazards, or loss of accessibility to the school or change of function as shelters.

A generic form of Bayesian network for a school infrastructure network is developed to study the disruption to education as shown in Figure 2. Three branches of the network correspond to the three main factors of the system contributing to the overall performance, namely physical functionality, functionality reduction from accessibility loss and social vulnerability. Branch 1 correlated hazard intensities to physical fragility of buildings and functionality disruption due to physical damage. Functionality loss from accessibility loss is captured through Branch 2, while social vulnerability indicators are connected through Branch 3. Assumed states of these variables are listed in Table 1. The nodes and arrows shown in the Figure 2 are representative of the infrastructure at system level. In reality, each node is repeated for the number of schools in the system, except for the hazard input nodes and the system output nodes (marked in red). For example, in a network of *n* schools, the node *DB* (inundation duration in the basin) is a cluster of *n* nodes (DB_1 *to* DB_n) corresponding to states of this parameter in each school, contributing to the 'shelter function' (SH_1 *to* SH_n) of respective schools. The output nodes 'overall disruption' and 'system disruption with SV' combine the states of individual schools to the system state.

The two root nodes, 'Earthquake' and 'Flood' represent the discretised probability distribution of hazard in terms of an intensity measure PGA for earthquake and inundation depth for flood. Earthquake and flood hazard curves for Guwahati are gathered from Nath and Thingbaijam (2012) and Sahoo and Sreeja (2008) respectively. The exact location of the schools are not specified in these networks, that enables to retain the generic nature of the analysis for schools in this study area under the same hazard intensity. Variability in accessibility to schools is incorporated through the assumed probability of flooding at the school site and the basin where the school is located. These features can be fine-tuned for a more specific case study, where the schools are specified by location. Hazard nodes lead to loss of physical functionality disruption to various states, as grouped within **Branch 1** or the green box in Figure 2. This box of variables further expand to a prior network, involving fragility curves for different building typologies under combined loading scenarios and

associated functionality loss of buildings. Components of this prior network analysis are discussed in the first subsection below.

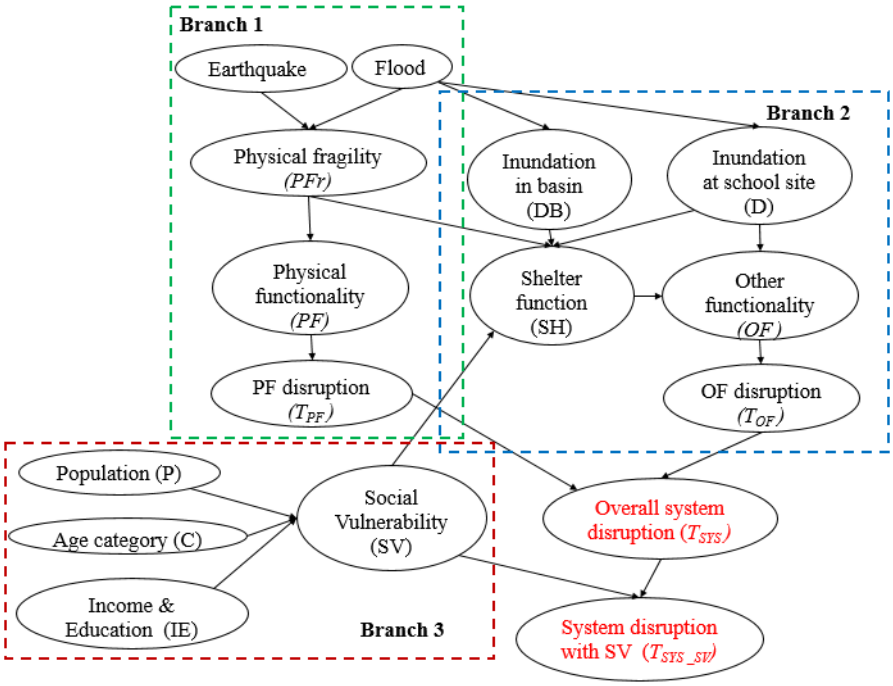

Figure 2 *Bayesian Network for the overall disruption to school system exposed to sequential hazards*

Branch 2 (blue box in Figure 2 further detailed in the second subsection) estimates the functionality disruption from causes other than physical functionality loss. In this study, this segment of non-structural duration of disruption is considered dependent on two factors: duration of flood inundation at the school's location accounting for local hydrology and topography (*D*), and the eventuality of the school being assigned shelter function (*SH*) for people affected by the events. While the first factor relates to accessibility, the second is a social variable, in turns depending on many other factors. Among various physical and social aspects qualifying the suitability of a school to be used as a shelter (Tsioulou et al. 2021), physical robustness and accessibility are considered in this study, as they are reciprocal to the variables states determining the school's loss of functionality. Therefore, *SH*, is a function of *PF* and *D* (as defined above). Moreover to capture the role of school-shelters in the community, the duration of inundation in the basin where school is located, *DB*, represents the probability of the residential areas served by school, of being flooded for a given period of time, hence needing shelter. Such need will also be conditional to the social vulnerability (*SV)* of the community relying on school-shelter.

Indicators of social vulnerability are linked in **Branch 3** of the network and the influence of social vulnerability in the education delivery to estimate overall disruption to the school system. It is noted that a multitude of factors affect the social vulnerability of a community and it affects the education process in a mutually dependent manner. However, to limit the scope of this study, three factors are considered here to estimate the social vulnerability of the school infrastructure, namely, size of student population (*P*) and category of school (*C*) based on age group of students and the state income and education (*IE*) of the community, as discussed in the third subsection below.

The probability of disruption related to physical and functional aspects of the school system as defined in Branches 1 and 2, is quantified in terms of the T_{SYS} variable. The system's overall disruption is also dependent on the effect of social vulnerability, quantified by the node T_{SYS_SV}. These two output nodes enable the comparison of disruption to education by considering only the physical and functionality aspects, and by considering the social vulnerability aspect. The following subsections detail the CPT definitions of each part of the network and the overall system.

Table 1 *States of variables in the Bayesian network*

Variables in the network	Assigned states (Assigned probabilities of root nodes are given in brackets)
	Branch 1
Earthquake	20 PGA states and their probabilities as defined by the earthquake hazard curve.
Flood depth	5 flood depth values and their probabilities defined by the flood hazard curve.
Physical fragility *(PFr)*	1. No damage 2. Immediate Occupancy 3. Life Safety 4. Collapse Prevention
Physical functionality loss at school level *(PF)*	1. Intact: minimal disruption, under1 week 2. Partially functioning: up to 3 months 3. Shutdown: 1 year
PF disruption at system level (T_{PF})	1. Short functionality loss under 1 week and minimal disruption 2. Medium functionality loss up to 3 months 3. Long functionality loss up to 12 months
	Branch 2
Duration of flooding at school site (*D*)	1: No inundation 2: 1-2 days 3: 3-6 days 4: 7-10 days
Duration of flooding in the basin (*DB)*	1- No inundation in basin 2-Inundation up to 1-2 weeks 3-Inundation up to 3-4 weeks (1 month)
Shelter function of school (*SH)*	1: not used as shelter 2: Used as shelter for up to 2-3 weeks 3: Used as shelter for up to 1-2 month 4: Used as shelter for up to 3-4 month (longer recovery)
Other functionality loss at school level *(OF)*	1: Negligible: under 1 week 2: Disruption for 2-3 weeks 3: Disruption for 1-3 months 4: Disruption for 4-12 months
OF disruption at system level (T_{OF})	1: Short: 'Low' disruption up to 3 weeks 2: Medium: 'Medium' disruption up to 3 months 3: Long: 'High' disruption up to 12 months
	Branch 3
Population (P)	1-0-50 students (0.1*) 2-50-100 students (0.3*) 3->100 students (0.6*)
Category of school (C)	1: LP school : class 1 to 5 (0.56*) 2: ME school: class 6-8 (0.22*) 3: HS school: class 9-10 (0.22*)
Income and Education of Parents (IE)	1-Above average (0.3**) 2-Average (0.4**) 3-Below average (0.3**)
Social vulnerability (*SV*)	1-Low vulnerability 2-Medium vulnerability 3-High vulnerability
	Overall System
Overall system disruption (T_{SYS}) and System disruption with SV (T_{SYS_SV})	1: Short: 'Low' disruption up to 3 weeks 2: Medium: 'Medium' disruption up to 3 months 3: Long: 'High' disruption up to 12 months

*(*Assigned probability based on field survey statistics, ** Assigned probability based on census data)*

Branch 1 - The sub-BN for disruption due to school's physical functionality (*PF*) level

Each school compound comprises multiple building blocks of different construction typology, hosting single or multiple functions, such as classroom, office, refectory, etc., and it can therefore be considered as a sub-system within the school infrastructure system. A specific BN is generated to estimate the functionality of each school compound and of a system of three compounds as shown in Figure 3. For this study, all buildings are assumed to be of the index building typology and all schools are assumed to have the same configuration of two building blocks performing three basic 'building functions' of the school, i.e. classroom, office and refectory. Nodes *Building 1* and *Building 2* input the fragility curves of the buildings to the network, corresponding to the earthquake and flood hazard intensities. CPTs of *Function* nodes are derived with respect to the fragility state of the building/s hosting that function: i) *no damage* and *immediate occupancy* correspond to unaffected functionality, ii) *collapse prevention* correspond to functionality total loss, iii) all other combinations of fragility states correspond to partially functional. The nodes *PF*, represents the physical functionality of the school as a system, assuming three possible states of disruption, conditional to the states of *Function* nodes as shown in Table 2. The inferred probabilities for each state of the *PF* nodes are carried forward to Branch 2 of the network, to assess the suitability of using the school as a shelter.

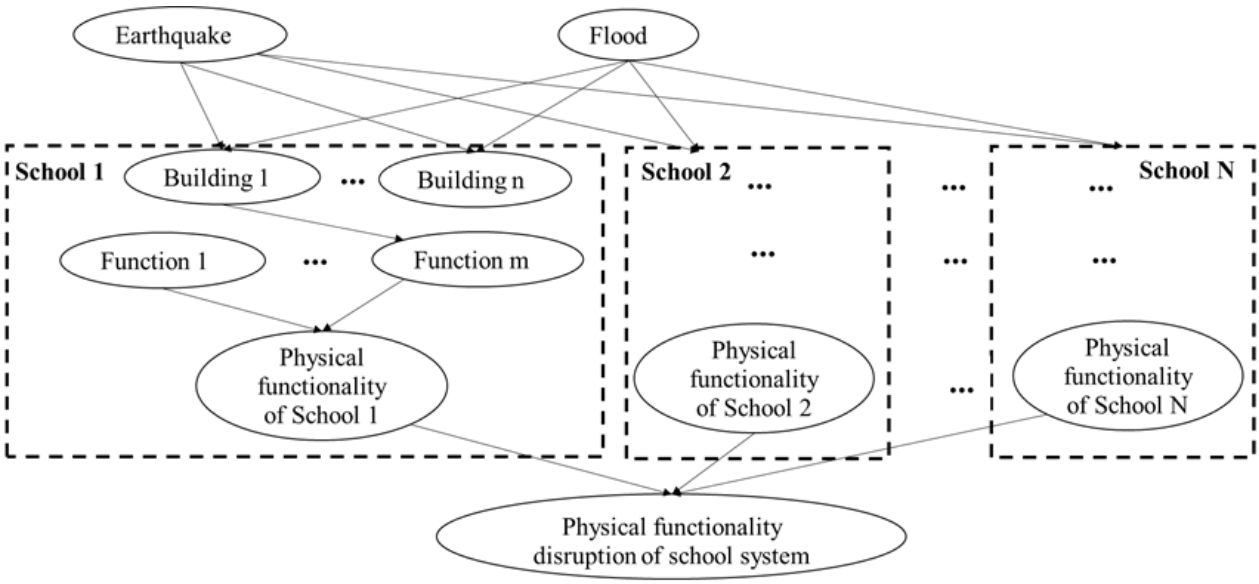

Figure 3 *Sub-BN for Branch 1: Schools' physical functionality network*

The output of Branch 1 subsystem is given by node T_{PF}, measuring the disruption to its physical functionality in terms of duration of recovery, whose CPT is obtained by combining the probabilities of individual school functionality states. Of the three possible states, if the damage level is beyond immediate occupancy, but not reaching life safety, it is expected to cause up to 3-4 months of recovery time, translating to a system performance state of 'partially functioning'. Such a recovery period implies options of rapid repair and rehabilitation such as the ferrocement technique (Dixit et al. 2013). Physical damage corresponding to the life safety threshold would require major structural repair, and 1 year is considered as a reasonable time period. The T_{PF} node is an input to the overall system disruption period 'T_{SYS}', as shown in Figure 2.

Table 2 *Conversion of functionality state to individual school functionality state*

Building Function	**Physical Functionality state (node *PF*)**
All *Function* nodes in fully functional state (state 1)	Intact (1)
All *Function* nodes are in shutdown state (state 3)	Shutdown (3)
All other combinations	Partially functional (2)

Branch 2: Disruption from other causes

Branch 2 evaluates the probability of different states of duration of disruption to education for individual schools from other causes of functionality loss (*OF*), i.e. other than the functionality loss induced by physical damage. These include the lack of accessibility due to inundation at the site of school and its basin, or the change in use, from educational to shelter or other post event function. The CPTs of duration of inundation at the school site (*D)* are derived from the flood depth hazard states, defined in number of days as per evidence provided by Sahoo and Sreeja (2008), in absence of systematic spatial data on flood depth and duration across the case-study location. Four states are assigned to *D*, linked to the five states of flood depth given by the hazard curve. The duration of inundation in the basin *(DB)*, also linked to flood depth, is defined in weeks rather than days as per evidence provided by Chakraborty and Singh (2016). *D* and *DB* allow to differentiate the accessibility of the school site from the state of inundation of the community, reflecting diverse topographic and hydrological features of the area under study. The state of these two variables determine the possible state of the school-shelter.

The *SH* has four states, ranging from 'not used as a shelter' to 'used as shelter up to four months'. Besides *D* and *DB*, the other two parent nodes determining *SH* states are the school functionality *PF* and the state of social vulnerability of the community *SV*. For instance, the school is more likely to be used as a shelter if the basin is inundated, but the location of school is not, owing to its high altitude or better drainage system, and if its functionality from Branch 1 is satisfactory. A high state of social vulnerability also increases the probability of the school being used as a shelter for extended period, while the community recovers. Table 3 provides the CPT of possible states of *SH* as a function of the states of its parent variables. Uniform probability distribution applies to all states.

Table 3 *CPT for SH node, conditioned on states of PF, D, DB and SV (corresponding states of the variable in brackets)*

PF	***D***	***DB***	***SV***	***SH* state**	**Combination rule**
shutdown (3)	more than 2 days of inundation at school site (3,4)			not used as a shelter (1)	OR
intact or partially functional (1,2)	less than 2 days of inundation at school site (1,2)	inundation up to 2 weeks in basin (2)	Low or medium level	used as shelter up to 3 weeks (2)	AND
			High level	used as shelter up to 2 months (3)	
intact or partially functional (1,2)	less than 2 days of inundation at school site (1,2)	inundation up to 4 weeks in basin (3)	Low or medium level	used as shelter for up to 2 months (3)	AND
			High level	used as shelter for up to 4 months (4)	

The CPT of individual school's disruption period from other functionality loss (*OF*), therefore is derived considering the correlation between duration of inundation at school site and shelter function of schools. Four possible states are defined for the disruption period (see Table 1) considering the following possible combinations of the parent nodes states:

- The school not being used as a shelter and inundation at site being minimum (*D* state 1 or 2), the non-structural disruption is under one week (*OF* state 1).
- The school's *SH* has the longest duration (up to 4 months) leads to a disruption period of up to 12 months *(OF* state 4), irrespective of the inundation at site.
- Other combinations of *D* and *SH* states lead to duration of disruption of 2 to 3 weeks or 1 to 3 months.

The overall disruption time T_{OF} for the school from non-structural causes is then defined applying combination rules, such that, the condition of all schools under 3 weeks of disruption is considered to cause an overall 'short' disruption of the education system. All schools up to a maximum of 3 months disruption leads to a 'medium' disruption of the system, while all other combinations lead to 'long' disruption, as at least one school will be facing 4-12 months of disruption individually.

Branch 3- Social vulnerability to flood and seismic hazards

Socioeconomic and demographic factors are together referred to as social vulnerability (Flanagan et al. 2011). Several studies quantify social vulnerability through summative indices that capture the states of the influencing factors (Armaș and Gavriș 2013; Willis and Fitton 2016; Tascón-González et al. 2020). However, it is shown that while these index-based studies help assess the social vulnerability, they are often subjective as to the weights assigned to each factor and the outcome can vary significantly when applied to a common case study (Willis and Fitton 2016).

This study considers four factors to describe the social vulnerability of the community associated with the school system under analysis. Two factors are school-specific: the size of student population (*P*), representing the exposure factor and the category of school (*C*) based on the age group of students, which relates directly to their vulnerability in an hazard event. Three states and their probabilities are assigned for each of these nodes based on the statistics of schools surveyed (Table 1). Studies have shown that low income and low levels of education are to an extent correlated (Utami 2019). Hence, social vulnerability of the community is accounted via the combined income and education (*IE*) of the parents of students in the area, for which three possible states and associated probabilities (Table 1) are based on the 2011 census of India. The census estimates a literacy rate of 73.18% , and a proportion of the population below the poverty line of 34% for Assam (MMA 2001; DES 2012, 2018). Given the poor resolution of this indicator *IE* is assumed as common value to all schools in one locality. The CPT of *SV* are defined considering the *P* and *C* states of individual schools, and the common *IE* state of the community, following the assumption that the larger the school population and the lower the children age attending a school compound, the higher the social vulnerability of the individual school's student population, amplified by poorer state of income and education of the community. Therefore:

1. Highest population or lowest age category when combined with the poorest income-education state lead to *high SV* ;
2. When *P* and *IE* are either 1 or 2 and *C* is either 2 or 3 (see Table 1) indicating low vulnerable conditions, the *SV* state is *low*;
3. All other combinations lead to a state of *medium* social vulnerability.

The social vulnerability of individual schools contributes to the level of social vulnerability of the overall school network. The CPTs of the overall system's social vulnerability states are defined by the combination of multiple schools being in any given state.

Overall System disruption

The 'impact' of combined hazards on the school system and the delivery of the education can be quantified as the *Overall Duration of Disruption* to the education system (T_{SYS}) (Figure 2) which is obtained as the combined product of the conditional probabilities of disruption due to schools' physical functionality (Branch 1-T_{PF}) and other functionality losses (Branch 2-T_{OF}). T_{SYS} is then modified by the level of social vulnerability (Branch 3) providing a *Modified Probability of Duration of Disruption*, T_{SYS_SV}. Both T_{SYS} and T_{SYS_SV} have three states, *short*, *medium* and *long* disruption. The CPT of T_{SYS} is defined with the following criteria:

- For the overall system to receive *short disruption* both parents should be in *short disruption* state, i.e. T_{PF} is within *1 week* and T_{OF} is limited to *under 3 weeks*.
- On the other hand, T_{SYS} will receive *long disruption, hence high impact*, if either of the two parent nodes are in *long disruption* state, i.e. T_{PF} or T_{OF} is *up to a year*.
- In all other combinations, the overall system is in *medium disruption or impact* state, up to 3 months.

CPT of T_{SYS_SV} is defined by considering the observation that children from highly vulnerable communities are more likely to miss schooling even when other physical and functional aspects of schools are undisturbed or brought back to normal after an event. To incorporate this into the BN, CPT of T_{SYS_SV} assumes that the state of overall disruption, $T_{SYS,}$ increases from *short* to *medium* and *medium* to *long*, if the SV state is '*high*'. Implications of '*low*' SV state to possibly reduce the long disruption period from other physical and functional causes is not explored in this analysis, due to lack of evidence to quantify this link.

RESULTS AND DISCUSSION

The Bayesian network illustrated in the previous section is applied to a system of 3 schools with the following simplifying assumptions: the analysis considers only one specified index building type for the general discussion on the probability and duration of disruption to the system, hence all buildings are assumed to be of this typology. Without loss of generality, identical prior probabilities and CPTs are assigned to variables across schools, such as *P, C, IE* etc., effectively assuming the same condition for all the schools. The results are presented in terms of the probability of disruption states for 1) the overall system disruption due to physical and other (non-structural) functionality loss, T_{SYS} and 2) the modified overall system disruption due to the community social vulnerability, T_{SYS_SV}. Three states of these variables short, medium and long duration of disruption, namely DD_s, DD_m and DD_l respectively, are considered. Furthermore, the influence of parent nodes on the system disruption states is assessed by means of a sensitivity study using the one-at-a-time (OAT) approach and by defining possible realistic scenarios.

Probability distributions of disruption to school system

The resulting probabilities of the states of disruption variables as a function of flood and seismic hazard intensities are presented in Figure 4. Probability distributions of two parent nodes of the first system output variable, T_{SYS} , i.e. T_{PF} and T_{OF} are shown in Figure 4a and b, respectively. Disruption states from the physical functionality reduction (T_{PF}) varies predominantly with seismic hazard intensities, as the influence of flood hazard intensities on the structural damage is limited. The 100% probability of DD_s from structural causes, at nil seismic intensity, rapidly decreases with increase in PGA, and becomes insignificant beyond 0.52g PGA, while a DD_m of up to 3 months becomes the most probable (95%) state for the system. The probability of DD_l up to 1 year increases gradually with PGA, with a maximum of 7.5% at the highest considered PGA, due to its low probability of occurrence, as per the hazard probability function used.

On the other hand, disruption from non-structural functionality loss T_{OF}, measuring the disruption from accessibility loss and change of function to shelter, is more dependent on the flood hazard level. Over the range of flood intensity considered, the probability of DD_s drops to a minimum of 48%. It can be noted that the probability of *short and long disruption* from non-structural causes show modest variation over the range of PGA, correctly capturing that the increased structural damage associated with PGA renders the schools unsuitable for shelter function. Therefore the probability of the 3 different states of overall disruption of the system, shown in Figure 4a, combines the independent trends of T_{PF} and T_{OF}, delivering short, medium and long disruption probabilities of 0.01%, 85.34% and 14.66 % respectively, for the coexisting maximum value of the two hazards.

Figure 4d presents the modification in the distribution of system disruption, by considering the effect of social vulnerability (T_{SYS_SV}). Given the probability distributions assigned to the root variables *IE, C* and *P* , the DD_s reduces to 70% in absence of hazardous events, with a corresponding rise of 30% in the DD_m, when compared to the T_{SYS}. This is due to considering the social vulnerability (*SV)* as a hazard independent component. The most relevant result is that DD_l probability for the maximum value of the two hazards is 2.5 times higher than the baseline case. This comparison of T_{SYS} and T_{SYS_SV} illustrates the sensitivity of the system to social vulnerability and highlights its influence for successful education delivery.

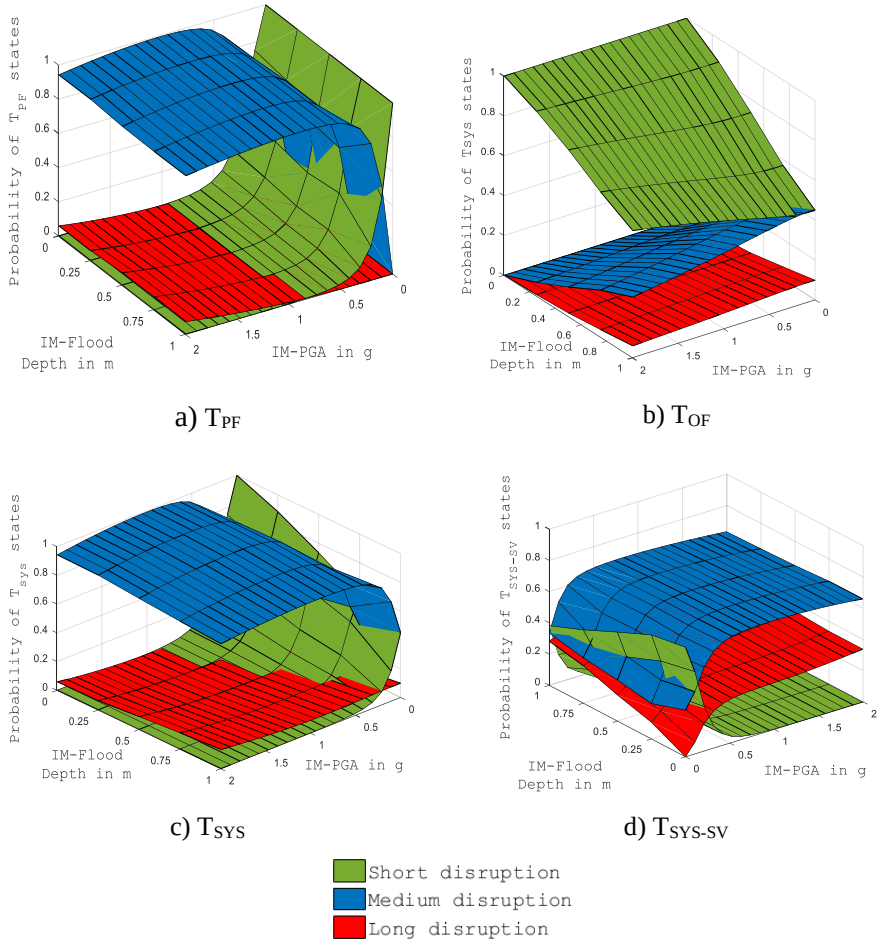

Figure 4 *Probability of T_{SYS} and T_{SYS_SV} states for a network of three schools*

Sensitivity of system variables to contributing factors

The influence of the contributing parameters on system's disruption duration can be studied by setting the states of some parent nodes to a desired value and computing the updated probabilities of output variables. In order to illustrate the sensitivity of the system disruption variable T_{SYS} through Bayesian inference, the estimated marginal probabilities of its three states is computed for three scenarios of practical significance:

1. One school's physical functionality after an event is (a) intact, possibly due to structural interventions prior to the event (i.e. *PF* state =1) and (b) shutdown, possibly due to structural damage during the event (i.e. *PF* state =3)
2. One school is (a) not used as a shelter (i.e. *SH* state =1) and (b) used as a shelter for over 3 months (i.e. *SH* state=4)
3. One school's inundation status is (a) not inundated, due to higher elevation (i.e. *D* state =1) and (b) inundated for more than a week (i.e. *D* state =4)

These evidence cases are provided to the BN to estimate the revised marginal probability over the flood hazard range at the PGA level of MCE, as shown in Figure 5. The originally estimated marginal probabilities of T_{SYS} without evidence are included, showing that under the given hazard characteristics, T_{SYS} has about 15% and 85% probability of being in DDs_s and DD_m, while a non-zero probability of DD_l exists. T_{SYS} shift for the 'case a' evidences for the three scenarios, i.e. state 1 for *PF*, *SH* and *D* are indicated by green markers in Figure 5 the red markers indicating the change caused by 'case b' evidence. For the first scenario (Figure 5), *PF* = 1 improves the probability of DD_s by 86%, while *PF* = 3 leads to 99% probability of DD_m. Under scenario 2, *SH* = 1 does not alter the original estimate significantly, but SH_1 = 3, produces a shift of T_{SYS} to DD_l, owing to the conditional probability definitions of *OF*. The duration of inundation at school site, *D* has modest influence on the original estimate of T_{SYS}, compared to the other two factors, due to its limited control over *OF* states,

and hence that of T_{SYS} states as defined by CPT of *OF*. It can be concluded that the *SH* state, which is also dependent on the *PF* state has a dominating influence on the states' probability of T_{SYS}.

Figure 5 *Influence of physical functionality, shelter function and inundation at site on duration of disruption of the school system (T_{SYS})*

CONCLUSION

In response to the need for estimating the effects of combined hazards on disruption of school systems, a Bayesian network model is proposed in this paper, by mapping the complex probabilistic impact assessment of a system of several schools exposed to dual hazards scenarios, in terms of duration of disruption of system functionality. The framework includes functionality loss due to physical fragility of the assets, accessibility of the compounds, changes in use to shelter, social vulnerability of the users' community and student population. The analysis illustrates that BN is suitable to model the multi-hazard resilience assessment problem, containing qualitative and quantitative information. In particular the inclusion of variables representing the social status of the users' community allows to quantify the relevance of social vulnerability, even though this is represented in a simple and qualitative way.

The results are limited by the availability of specific elements of data, from the modest characterisation of the hazards, to the lack of resolution of the social variables. Nonetheless, the methodology is robust and allows to account for and propagate the uncertainties through the system enabling a probabilistic assessment of the disruption to the system. More nuanced results can be obtained with better data resolution, such as detailed flood basin characteristics, student demographics, seismicity at the sites, etc. The study illustrated the analysis results of a system containing three schools computationally very efficient. However, the challenge of extending the network for a large number of schools in a full regional network, while feasible needs further exploration with respect to computational optimisation.

REFERENCES

Akello S (2014) Effects of floods on students access to secondary education in Nyando district, Kisumu county, Kenya. University of Nairobi

Alcocer SM, Arce JC, Murià-Vila D, et al (2020) Assessment of the seismic safety of school buildings in Mexico: A first look. Earthq Spectra 36:130–153. https://doi.org/10.1177/8755293020926184

Anderson A, McFarlane K, Petal M, Moli S (2017) Limiting and planning for schools as temporary evacuation centres in emergencies: Policy brief and practice guidance for pacific nations in support of the Worldwide Initiative for Safe Schools. Asia Pacific Coalition for School Safety

Ardales GY, Victoria Espaldon MO, Lasco RD, et al (2016) Impacts of floods on public schools in the municipalities of

Los Baños and Bay, Laguna, Philippines. J Nat Stud 15:19–40
Armaș I, Gavriș A (2013) Social vulnerability assessment using spatial multi-criteria analysis (SEVI model) and the Social Vulnerability Index (SoVI model) – a case study for Bucharest, Romania. Nat Hazards Earth Syst Sci 13:1481–1499
Bayraktarli YY, Ulfkjaer J, Yazgan U, Faber MH (2005) On the application of Bayesian probabilistic networks for earthquake risk management. In: 9th International Conference on Structural Safety and Reliability (ICOSSAR 05). pp 20–23
BBC (2015) Chennai schools reopen after floods. https://www.bbc.co.uk/news/world-asia-india-35090145
Bensi MT (2010) A Bayesian Network Methodology for Infrastructure Seismic Risk Assessment and Decision Support (Thesis). University of California, Berkeley
Bertho A, Pande D, Shrichand P, Singh S (2012) Impact of Disasters on Children : A Case Study of Five Disaster-Prone Districts in Uttar Pradesh and Bihar , India. Knowledge Community of Children in India
Brzev S (2007) Earthquake-Resistant Confined Masonry Construction, NICEE. National Information Center of Earthquake Engineering
Chakraborty D, Singh M (2016) Development and urban Flooding, Case-Guwahati. J Basic Appl Eng Res 3:1081–1086
Choudhury CP, Pathak J (2014) Analytical study of seismic response of traditional Assam-type housing in north-east India. In: 15th Symposium on Earthquake Engineering. IIT Roorkee
Chourasia A, Bhattacharyya SK, Bhandari NM, Bhargava P (2016) Seismic performance of different masonry buildings: full-scale experimental study. J Perform Constr Facil 26:371–376. https://doi.org/10.1061/(ASCE)CF
Chourasia A, Bhattacharyya SK, Bhargava PK, Bhandari NM (2013) Influential aspects on seismic performance of confined masonry construction. Nat Sci 05:56–62. https://doi.org/10.4236/ns.2013.58a1007
D'Ayala DF, Galasso C, Putrino V, et al (2016) Assessment of the multi-hazard vulnerability of priority cultural heritage structures in the Philippines. In: ICONHIC. Chania, Greece
de Ruiter MC, Couasnon A, van den Homberg MJC, et al (2020a) Why we can no longer ignore consecutive disasters. Earth's Futur 8:. https://doi.org/10.1029/2019EF001425
de Ruiter MC, de Bruijn JA, Englhardt J, et al (2020b) The asynergies of structural disaster risk reduction Measures: comparing floods and earthquakes. Earth's Futur. https://doi.org/10.1029/2020EF001531
de Ruiter MC, Ward PJ, Daniell JE, Aerts JCJH (2017) Review Article : A Comparison of Flood and Earthquake Vulnerability Assessment Indicators. Nat Hazards Earth Syst Sci 1–34. https://doi.org/10.5194/nhess-2017-45
DES (2018) Economic Survey Assam 2017-18. Government of Assam
DES (2012) Economic Survey Assam 2011-12. Directorate of Economics and Statistics. Government of Assam
Dixit AM, Yatabe R, Dahal RK, Bhandary NP (2013) Public school earthquake safety program in Nepal. Geomatics, Nat Hazards Risk 5:293–319. https://doi.org/10.1080/19475705.2013.806363
Doocy S, Daniels A, Murray S, Kirsch TD (2013) The human impact of floods : a historical review of events 1980-2009 and systematic literature review. PLOS Curr Disasters 1–30. https://doi.org/10.1371/currents.dis.f4deb457904936b07c09daa98ee8171a.Authors
ELS (2004) Extreme Loading ® for Structures Theoretical Manual, Applied Science International, LLC
Fajfar P (2000) A non-linear analysis method for performance-based seismic design. Earthq Spectra 16:573–592
Fatemi F, Ardalan A, Aguirre B, et al (2017) Social vulnerability indicators in disasters : Findings from a systematic review. Int J Disaster Risk Reduct 22:219–227. https://doi.org/10.1016/j.ijdrr.2016.09.006
Flanagan BE, Gregory EW, Hallisey EJ, et al (2011) A social vulnerability index for disaster management. J Homel Secur Emerg Manag 8:. https://doi.org/10.2202/1547-7355.1792
Forino G, Meding J Von (2018) Child-Centred Risk Reduction Research-into- Action Brief: Post-Disaster Educational Continuity in Urban Floods. Global Alliance for Disaster Risk Reduction & Resilience in the Education Sector
Franchin P, Lupoi A, Noto F, Tesfamariam S (2016) Seismic fragility of reinforced concrete girder bridges using Bayesian belief network. 29–44. https://doi.org/10.1002/eqe
Gehl P (2017) Bayesian Networks for the Multi-Risk Assessment of Road Infrastructure (Thesis). University College London, UK
Herbert DM (2013) An investigation of the strength of brickwork walls when subject to flood loading (Thesis). Cardiff University
Herbert DM, Gardner DR, Harbottle M, Hughes TG (2012) The strength of masonry walls when subject to flood loading. In: 15th International Brick and Block Masonry Conference
Huang S, Wang H, Xu Y, et al (2021) Key disaster-causing factors chains on urban flood risk. MDPI L 10:. https://doi.org/https:/doi.org/10.3390/land10020210
IS1893 (2002) Indian Standard: Criteria for earthquake resistant design of structures, Bureau of Indian Standards
Kaushik HB, Rai DC, Jain SK (2007) Stress-Strain Characteristics of Clay Brick Masonry under Uniaxial Compression. J Mater Civ Eng 19:728–739. https://doi.org/10.1061/(ASCE)0899-1561(2007)19:9(728)
Kelman I, Spence R (2003) A limit analysis of unreinforced masonry failing under flood water pressure. Mason. Int. 16:51–61
Meli R, Brzev S, Astroza M, et al (2011) Seismic design guide for low-rise confined masonry buildings. Earthquake Engineering Research Institute, Oakland, California
Milanesi L, Pilotti M, Belleri A, et al (2018) Vulnerability to flash floods: A simplified structural model for masonry

buildings. Water Resour Res 7177–7197. https://doi.org/10.1029/2018WR022577
Miyamoto HK, Gilani ASJ (2017) Damage assessment and seismic retrofit of heritage and modern buildings in the aftermath of 2015 Nepal Earthquake. In: 16th WCEE. Santiago, Chile
MMA (2001) District Report Kamrup. Ministry of Minority Affairs Government of India
Mudavanhu C (2014) The Impact of Flood Disasters on Child Education in Muzarabani District, Zimbabwe. J Disaster Risk Stud 6:1–8
Munsaka E, Mutasa S (2020) Flooding and its impact on education. In: Natural Hazards-Impacts, Adjustments & Resilience-IntechOpen
Nath SK, Thingbaijam K (2012) Probabilistic Seismic Hazard Assessment of India. Seismol Res Lett 83:135–149. https://doi.org/10.1785/gssrl.83.1.135
Pathak J (2014) Status Survey of School & Hospital buildings in Guwahati city Vol II-Restoration and Retrofitting Advisory. Assam State Disaster Management Authority (ASDMA) Department of Civil Engineering, Assam Engineering College (AEC)
Pribadi KS, Abduha M, Wirahadikusumaha RD, et al (2021) Learning from past earthquake disasters: The need for knowledge management system to enhance infrastructure resilience in Indonesia. Int J Disaster Risk Reduction,
Reliefweb (2018) Hundreds of schools reopen after devastating floods in India. https://reliefweb.int/report/india/hundreds-schools-reopen-after-devastating-floods-india
Rodgers J (2012) Why schools are vulnerable to earthquakes. In: Proceedings, 15th world conference on earthquake engineering,. Lisbon
Sahoo SN, Sreeja P (2017) Development of Flood Inundation Maps and Quantification of Flood Risk in an Urban Catchment of Brahmaputra River. 3:1–11. https://doi.org/10.1061/AJRUA6.0000822.
Sen MK, Dutta S, Laskar JI (2021) A Hierarchical Bayesian Network Model for Flood Resilience Quantification of Housing Infrastructure Systems. ASCE-ASME J Risk Uncertain Eng Syst Part A Civ Eng 7:04020060. https://doi.org/10.1061/ajrua6.0001108
Simonovic SP (2003) Civil Engineering Systems- Course notes, The University of Western Ontario
Stephenson V, D'Ayala D (2019) Structural Response of Masonry Infilled Timber Frames to Flood and Wind Driven Rain Exposure. J Perform Constr Facil 33:. https://doi.org/10.1061/(ASCE)CF.1943-5509.0001281.
Tascón-González L, Ferrer-Julià M, Ruiz M, García-Meléndez E (2020) Social vulnerability vssessment for flood risk analysis. Water 12:. https://doi.org/10.3390/w12020558
Tomaževi˘c M, Weiss P (2010) Displacement capacity of masonry buildings as a basis for the assessment of behavior factor : an experimental study. Bull Earthq Eng 8:1267–1294. https://doi.org/10.1007/s10518-010-9181-y
Tomaževič M, Klemenc I (1997) Seismic behaviour of confined masonry walls. Earthq Eng Struct Dyn 26:1059–1071. https://doi.org/10.1002/(SICI)1096-9845(199710)26:10<1059::AID-EQE694>3.0.CO;2-M
Tsioulou A, Faure Walker J, Lo DS, Yore R (2021) A method for determining the suitability of schools as evacuation shelters and aid distribution hubs following disasters: case study from Cagayan de Oro, Philippines. Nat Hazards 105:1835–1859. https://doi.org/10.1007/s11069-020-04380-3
UN (2009) Reducing Vulnerability of School Children to Earthquakes, United Nations Centre for Regional Development (UNCRD)
UNISDR (2015) Sendai Framework for Disaster Risk Reduction 2015 - 2030. In: rr.org/uploads/Sendai_Framework_for_. http://www.wcdrr.org/uploads/Sendai_Framework_for_Disaster_Risk_Reduction_2015-2030.pdf
Utami W (2019) Study of social vulnerability as an effort on disaster risk reduction (study on suburban communities in Yogyakarta , Indonesia). IOP Conf Ser Earth Environ Sci 243 012014. https://doi.org/10.1088/1755-1315/243/1/012014
Vatteri AP, D'Ayala D (2021) Classification and seismic fragility assessment of confined masonry school buildings. Bull Earthq Eng. https://doi.org/10.1007/s10518-021-01061-9
Vatteri AP, D'Ayala D, Gehl P (2022) Bayesian networks for the assessment of disrption to school systems under combined hazards. Int J Disaster Risk Reduct (under rev)
Weber P, Medina-Oliva G, Simon C, Iung B (2012) Overview on Bayesian networks applications for dependability , risk analysis and maintenance areas. Eng Appl Artif Intell 25:671–682. https://doi.org/10.1016/j.engappai.2010.06.002
Willis I, Fitton J (2016) A review of multivariate social vulnerability methodologies: a case study of the River Parrett catchment, UK. Nat Hazards Earth Syst Sci 16:1387–1399
Wu Z, Shen Y, Wang H, Wu M (2019) Assessing urban flood disaster risk using Bayesian network model and GIS applications. Geomatics, Nat Hazards Risk 10:2163–2184. https://doi.org/10.1080/19475705.2019.1685010